Proceedings of the 2001 IEEE
International Conference on Robotics & Automation
Seoul, Korea · May 21-26, 2001

Dynamics and Control of Whole Arm Grasps

Peng Song Masahito Yashima Vijay Kumar

General Robotics, Automation, Sensing and Perception (GRASP) Laboratory
University of Pennsylvania, 3401 Walnut Street, Philadelphia, PA 19104
E-mail: {pengs, yashima, kumar}@grasp.cis.upenn.edu

Abstract

In this paper we consider the dynamics and control of whole arm grasping systems. We develop a control scheme that employs a minimal set of inputs to control the trajectory of the system while using the surplus inputs to control the interaction forces in order to maintain the unilateral constraints at both rolling and sliding contacts. Since the number of surplus inputs is less than the number of output force variables, we propose a controller that controls the critical contact force components. We emphasize the dynamic models and algorithms for computing contact forces, which are crucial to the development of the control algorithms. Finally, we show how compliant contact models and a previously developed integrated simulation approach [14] are used to overcome the difficulties with uniqueness and existence of solutions. A planar whole arm manipulation system is used as an example to illustrate the basic ideas.

1 Introduction

There are many tasks that require whole arm grasps, such as restraining large objects, lifting heavy loads or assembling mating parts. In contrast to fingertip grasps, whole arm grasps are formed by wrapping the arms (or fingers) around the objects. The key features in such systems include (1) the closed chain structure that imposes the kinematic and dynamic constrains on the control equations; (2) the unilateral constraints brought by rigid body contacts; and (3) the redundancy in the actuation. These features are also shared by systems such as multi-fingered grippers [4], legged locomotion systems [9], and other constraint robot systems [12]. In addition, however, in contrast to finger tip grasps, it is generally not possible to control all the grasp constraint forces. A variety of control schemes for motion control and hybrid control have been developed for similar systems [2, 8]. Bicchi *et al.* studied the kinematics of general whole arm manipulation systems and discussed their manipulability [1]. Cole *et al.* derived the motion control algorithms for multi-fingered hands with rolling [3] and sliding [4] contacts but their controller is open loop for the force control part. Schemes for simutaneously controlling both motion and internal forces are described in [7, 12, 18]. But the control algorithms require that the fingers or the manipulator grippers are rigidly attached to the object. The contacts are treated in a similar fashion as the bilateral constraints. A virtual truss model is proposed in [17] to model internal force and to build the close loop force control algorithm. In contrast to these papers, our focus here is to maintain the contact forces at a threshold value when the number of contact forces is greater than the number of surplus inputs.

Further, models for contact force and algorithms for forward dynamics simulation, while crucial to the development of control algorithms and the design of such systems, have been largely overlooked in most of these research efforts. It is known that difficulties with uniqueness and existence arise when we compute the contact forces in the above mentioned systems by using classical rigid body models in conjunction with Coulomb's friction law [10, 15]. There has been some attention in the robotics community on resolving these difficulties by using rigid body models to predict the gross motion while using compliant contact models to predict the contact forces and the local deformations [11, 16]. But the compliant contact models can result in a high-dimensional, stiff system of equations and a run time that is unacceptable for real-time simulation. The simplicity and efficiency of rigid body models, on the other hand, provide strong motivation for their use during those portions of a simulation when the rigid body solution is unique and stable [13].

In this paper, we first develop a model based scheme that employs a minimal set of inputs to control the motion of the system while using the surplus inputs to regulate the interaction forces and to maintain the unilateral constraints at both rolling and sliding contacts. Since the number of surplus inputs is less than the number of output force variables in general, we propose a controller that controls the critical contact force components. We then describe and analyze models that explicitly compute the contact forces for the control algorithms and simulations. We use the integrated framework for dynamic simulation proposed in [14] to serve as a testbed for the design and evaluation of our control schemes. Finally we apply the basic ideas to the control and simulation of a planar whole arm manipulation system.

2 System dynamics

We consider a system of multiple rigid arms or effectors operating on rigid objects subject to Coulomb's friction as shown in Figure 1. The dynamic equations of motion can be written as

$$\boldsymbol{M}(\boldsymbol{q})\ddot{\boldsymbol{q}} + \boldsymbol{h}(\boldsymbol{q}, \dot{\boldsymbol{q}}) = \boldsymbol{u} + \boldsymbol{W}\boldsymbol{\lambda} \qquad (1)$$

where $\boldsymbol{q} \in \Re^n$ is the vector of generalized coordinates, $\boldsymbol{M}(\boldsymbol{q})$ is an $n \times n$ positive-definite symmetric inertia matrix, $\boldsymbol{h}(\boldsymbol{q}, \dot{\boldsymbol{q}})$ is a $n \times 1$ vector of nonlinear inertial forces,

$\boldsymbol{u}$ is the vector of applied (external) forces and torques, and $\boldsymbol{\lambda}$ is the vector of constraint forces. The system is subject to k unilateral constraints:

$$\boldsymbol{\phi}(\boldsymbol{q}) = [\phi_1(\boldsymbol{q}), \cdots, \phi_k(\boldsymbol{q})]^T \geq 0 \tag{2}$$

and $\boldsymbol{W}$ in Equation (1) is the $k \times n$ matrix derived from the Jacobian $(\frac{\partial \boldsymbol{\phi}}{\partial \boldsymbol{q}})^T$ with the consideration of Coulomb's law according to Equations (3) and (4) below. We will assume, without loss of generality, that this does not include bilateral, holonomic constraints. Further, for the sake of simplicity, we will assume that nonholonomic constraints are not present.

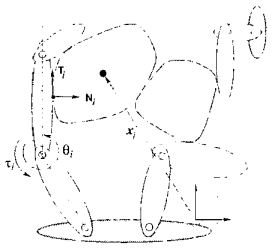

Figure 1: A general whole arm grasp.

Suppose there are n_C contacts, consisting of n_R rolling contacts and n_S sliding contacts. Let the subscripts N and T denote quantities in the normal and tangential contact directions and S and R denote sliding and rolling contacts respectively. The Jacobian matrix and constraint forces in Equation (1) are given by:

$$\begin{aligned} \boldsymbol{W} &= \left[\boldsymbol{W}_\mu \;\; \boldsymbol{W}_{NR} \;\; \boldsymbol{W}_{TR}\right], \qquad (3) \\ \boldsymbol{W}_\mu &= \left[\boldsymbol{W}_{NS} + \boldsymbol{W}_{TS}\boldsymbol{\mu}_s\right], \\ \boldsymbol{\lambda} &= \left[\boldsymbol{\lambda}_{NS}^T \;\; \boldsymbol{\lambda}_{NR}^T \;\; \boldsymbol{\lambda}_{TR}^T\right]^T, \qquad (4) \end{aligned}$$

where $\boldsymbol{\mu}_s = -diag(\boldsymbol{\mu}\, sign(\dot{\boldsymbol{\phi}}_{TS}))$, $\boldsymbol{\mu}$ is a $n_S \times n_S$ diagonal matrix that contains all the coefficients of friction at the sliding contacts, $\boldsymbol{W}_\mu$ is a $n \times n_S$ matrix, $\boldsymbol{W}_{NR}$ and $\boldsymbol{W}_{TR}$ are both $n \times n_R$ matrices, and the total number of constraints $k = 2n_R + n_S$. $\boldsymbol{\lambda}_{NS}$ is the n_S-dimensional vector of normal forces at sliding contacts, while $\boldsymbol{\lambda}_{NR}$ and $\boldsymbol{\lambda}_{TR}$ are the $n_R \times 1$ vectors of normal and tangential forces at rolling contacts, respectively.

For a typical manipulation system, the generalized coordinates can be chosen as $\boldsymbol{q} = [\boldsymbol{x}^T \;\; \boldsymbol{\theta}^T]^T$, where $\boldsymbol{x} \in \Re^{n_x}$ describes the position and orientation of object and $\boldsymbol{\theta} \in \Re^{n_\theta}$ be the joint angle of the robot manipulator. If Coulomb's friction law is assumed, we can rewrite Equation (1) to describe dynamics of the robot arms and the object separately. We define $\boldsymbol{G}_{N,i}$ and $\boldsymbol{G}_{T,i}$ as the unit wrenches associated with contact forces $\lambda_{N,i}$ and $\lambda_{T,i}$ respectively. The equations of motion for the object are given by

$$\boldsymbol{M}_o \ddot{\boldsymbol{x}} = \boldsymbol{G}\boldsymbol{\lambda} + \boldsymbol{g}_o, \tag{5}$$

where

$$\boldsymbol{G} = [\boldsymbol{G}_\mu \;\; \boldsymbol{G}_{NR} \;\; \boldsymbol{G}_{TR}] \in \Re^{n_x \times k}, \;\; \boldsymbol{G}_\mu = [\boldsymbol{G}_{NS} + \boldsymbol{G}_{TS}\boldsymbol{\mu}_s].$$

$\boldsymbol{M}_o$ is the mass matrix of the object and the vector $\boldsymbol{g}_o$ denotes the external wrench acting on the object. Let $\boldsymbol{J}_N^T$ and $\boldsymbol{J}_T^T$ be the arm Jacobians which map the normal and tangential contact wrenches to the joint torque $\boldsymbol{\tau}$, then the arm dynamics is given by

$$\boldsymbol{M}_a \ddot{\boldsymbol{\theta}} = \boldsymbol{\tau} - (\boldsymbol{J}^T\boldsymbol{\lambda} + \boldsymbol{h}_a + \boldsymbol{g}_a) \tag{6}$$

where

$$\boldsymbol{J}^T = \left[\boldsymbol{J}_\mu^T \;\; \boldsymbol{J}_{NR}^T \;\; \boldsymbol{J}_{TR}^T\right] \in \Re^{n_\theta \times k}, \;\; \boldsymbol{J}_\mu^T = \left[\boldsymbol{J}_{NS}^T + \boldsymbol{J}_{TS}^T\boldsymbol{\mu}_s\right].$$

$\boldsymbol{M}_a$ is the inertia matrix of the arm, $\boldsymbol{h}_a$ is the vector of Coriolis and centrifugal forces, and $\boldsymbol{g}_a$ represents the generalized forces that accounts for external forces acting on the arm. The $\boldsymbol{W}$ matrix in Equation (3) can be expressed in terms of the wrench matrix $\boldsymbol{G}$ and the robot Jacobian $\boldsymbol{J}$ as

$$\boldsymbol{W}^T = [\boldsymbol{G}^T \;\; -\boldsymbol{J}] \in \Re^{k \times n}.$$

3 Controller design

3.1 Model based control algorithm

The rigidity assumption and the contact conditions ensures the following relations on the relative velocities of the contact points:

$$\dot{\boldsymbol{\phi}} = [\boldsymbol{W}_{NS} \;\; \boldsymbol{W}_{NR} \;\; \boldsymbol{W}_{TR}]^T\dot{\boldsymbol{q}} = 0, \tag{7}$$

i.e.

$$\tilde{\boldsymbol{J}}\dot{\boldsymbol{\theta}} = \tilde{\boldsymbol{G}}^T\dot{\boldsymbol{x}},$$

where

$$\begin{aligned} \tilde{\boldsymbol{J}} &\triangleq [\boldsymbol{J}_{NS}^T \;\; \boldsymbol{J}_{NR}^T \;\; \boldsymbol{J}_{TR}^T]^T \\ \tilde{\boldsymbol{G}} &\triangleq [\boldsymbol{G}_{NS} \;\; \boldsymbol{G}_{NR} \;\; \boldsymbol{G}_{TR}]. \end{aligned}$$

We assume that the complete system is

1. statically determined – $\boldsymbol{W}$ is full rank; and
2. manipulable – there exists an unique set of the joint velocities $\dot{\boldsymbol{\theta}}$ to provide arbitrary instantaneous velocities for the contact points and the object [6].

The second assumption implies that $\tilde{\boldsymbol{G}}$ is full row rank and $\tilde{\boldsymbol{J}}$ is square and invertible. This in turn implies that $\boldsymbol{J}$ is invertible given that $\boldsymbol{W}$ is full rank. Therefore, we can express $\dot{\boldsymbol{\theta}}$ in terms of $\dot{\boldsymbol{x}}$ as

$$\dot{\boldsymbol{\theta}} = \tilde{\boldsymbol{J}}^{-1}\tilde{\boldsymbol{G}}^T\dot{\boldsymbol{x}} \triangleq \tilde{\boldsymbol{H}}\dot{\boldsymbol{x}}. \tag{8}$$

Now we use the velocity and acceleration constraints (by differentiating 8) to rewrite the system motion equations (5-6) in the operational space. First we decompose the contact force of the object in Eq.5 into equilibrating forces and internal forces.

$$\boldsymbol{\lambda} = \boldsymbol{G}^+(\boldsymbol{M}_o\ddot{\boldsymbol{x}} - \boldsymbol{g}_o) + \boldsymbol{\lambda}_I \tag{9}$$

where $\boldsymbol{G}^+ = \boldsymbol{G}^T(\boldsymbol{G}\boldsymbol{G}^T)^{-1}$ is the pseudo-inverse of the wrench matrix $\boldsymbol{G}$. $\boldsymbol{\lambda}_I$ is the internal force vector that lies in the null space of $\boldsymbol{G}$. If $\boldsymbol{G}^o \triangleq null(\boldsymbol{G})$ denotes the basis of the null space of $\boldsymbol{G}$, we can write

$$\boldsymbol{\lambda}_I = \boldsymbol{G}^o\boldsymbol{\alpha} \in \Re^{2n_R + n_S}$$

where $\boldsymbol{\alpha}$ is a $p \times 1$ vector of the internal force magnitudes or wrench intensities and p is the dimension of the null space $\boldsymbol{G}^o$. Combine equations (6) and (9) to obtain the following complete system dynamics equation:

$$\tilde{\boldsymbol{M}}(\boldsymbol{x})\ddot{\boldsymbol{x}} + \tilde{\boldsymbol{N}}(\boldsymbol{x}, \dot{\boldsymbol{x}}) + \boldsymbol{J}^T(\boldsymbol{x})\boldsymbol{G}^o(\boldsymbol{x})\boldsymbol{\alpha} = \boldsymbol{\tau}, \tag{10}$$

where $\tilde{M} = M_a\tilde{H} + (H^T)^+M_o$,
$\tilde{N} = M_a\dot{\tilde{H}}\dot{x} - (H^T)^+g_o + h_a$,
$H = J^{-1}G^T$.

Based on the complete system dynamics, we propose the following control law for simultaneous control of the object trajectory and the internal force magnitudes:

$$\tau = \tilde{M}(\ddot{x}_d + K_v\dot{e}_x + K_p e_x) + J^T G^o(\alpha_d + K_\alpha \int e_\alpha dt) + \tilde{N}. \quad (11)$$

The first term in the controller is a proportional and derivative error feedback term to regulate the motion of the object, in which $e_x \triangleq x_d - x$ is the position and orientation error, K_v and K_p are the feedback gain matrices. The second term is an integral error feedback term to control the magnitudes of the internal forces, where $e_\alpha \triangleq \alpha_d - \alpha$ and K_α is the feedback gain matrix. The third term is used for cancellation of gravitational, Coriolis, and centrifugal forces.

Theorem 3.1 *Consider a manipulation system described by Eq.(5) and (6), with proper choices of K_v, K_p, and K_α, the control law specified by Eq.(11) guarantees that both the object motion, $x(t)$, and the internal force magnitudes, $\alpha(t)$, converge to their preplanned trajectories, $x_d(t)$ and $\alpha_d(t)$, respectively.*

Proof: Substitute the control law (11) into (10) and premultiply H^T to yield

$$H^T\tilde{M}(\ddot{e}_x + K_v\dot{e}_x + K_p e_x) + H^T J^T G^o(e_\alpha + K_\alpha \int e_\alpha dt) = 0.$$

From the definition of H, we have that (12)

$$H^T J^T G^o(e_\alpha + K_\alpha \int e_\alpha dt) = 0$$

which results in

$$(H^T M_a \tilde{H} + M_o)(\ddot{e}_x + K_v\dot{e}_x + K_p e_x) = 0. \quad (13)$$

Since in general, the inertia matrix $(H^T M_a \tilde{H} + M_o)$ is nonsingular, Equation (13) implies that

$$\ddot{e}_x + K_v\dot{e}_x + K_p e_x = 0, \quad (14)$$

which shows that the trajectory tracking error goes to zero with appropriate selection of K_v and K_p. Combine (14) and (12) and notice that $J^T G^o$ has full column rank, we obtain

$$e_\alpha + K_\alpha \int e_\alpha dt = 0. \quad (15)$$

Again, with the proper choice of K_α, e_α goes to 0.

3.2 Planning the contact forces

Eq.(9) implies that as the internal force goes to the desired value, we can gain a certain level of control over the contact force through proper planning of the desired internal force magnitude vector α. But in our derivation thus far, we have not considered any restrictions on the contact forces. However, in order to apply the control law (11), the contacts between the arms and object have to be maintained and the Coulomb's friction law has to be satisfied as described by the following unilateral constraints:

$$\begin{aligned} \lambda_{N,i} &\geq 0 \\ \mu_i\lambda_{N,i} - |\lambda_{T,i}| &\geq 0 \end{aligned} \quad i = 1, \ldots, n_C. \quad (16)$$

This condition can be satisfied through the following planning of the internal force magnitudes, α_d.

$$\alpha_d = \min_{\alpha} \left(\sum_{i=1}^{n_C} \lambda_{N,i} + \sum_{i=1}^{n_R} (\mu_i \lambda_{n_S+i} - |\lambda_{n_C+i}|) \right)$$
$$\text{s.t. } \lambda = G^+(M\ddot{x}_d - g_o) + G^o\alpha \geq \Lambda \quad (17)$$

where Λ is a $(n_C + n_R) \times 1$ vector. The first n_C entries of Λ are positive scalars representing the desired trajectories of the minimum contact forces in the normal direction and the remaining components are zero.

(17) specifies the setpoint for α that maintains the unilateral constraints by keeping the normal contact force above a threshold. This same procedure is also used to maintain the rolling contacts. (16) can be augmented by other conditions if desired and (17) can be suitably modified to incorporate such conditions.

3.3 Discussion

In general, for a manipulation system with n actuators and mobility m, only m actuators (inputs) are required to control the motion of the system and $n-m$ actuators can be utilized to control the interaction forces. In most cases, the number of surplus inputs is less than the number of the unilateral constraints. The control algorithm developed here shows that, through the proper planning of the internal force magnitudes, the distribution of normal contact forces among all contacts can be controlled by using the limited surplus inputs.

Unlike the states variables $(x, \dot{x})$, the internal force magnitude α in the control law (11) can not be measured in general. It has to be obtained through Eq.(9) with the knowledge of the contact forces. In an experimental setup such as the one described in [7] the contact forces can be measured through force sensors. In the next section, we will develop a simulation frame work that enables the analysis and validation of control algorithms for whole arm grasps. This effort builds on our previous work [14] and integrates rigid body dynamic models with compliant contact models that allow the unique determination of contact forces.

4 Simulation approach

4.1 Contact models

LCP formulations Contacts between rigid bodies generate complementary constraints on the position (or velocity or acceleration) variables and the corresponding force variables. The question of whether there exists a unique solution for $\ddot{q}$ that is consistent with these constraints and Equations (1 - 4) and has been studied using complementarity formulations [10, 15]. The problem of determining contact forces can be reduced to a linear complementarity problem (LCP) that has the form [15]:

$$x \geq 0,\ y = Ax + b \geq 0,\ y^T x = 0. \quad (18)$$

For example, for a system with all sliding contacts,

$$\boldsymbol{y}=\ddot{\boldsymbol{\phi}}_{NS},\ \boldsymbol{x}=\boldsymbol{\lambda}_{NS},\ \boldsymbol{A}=\boldsymbol{W}_{NS}^{T}\boldsymbol{M}^{-1}\boldsymbol{W}_{\mu},$$
$$\boldsymbol{b}=\boldsymbol{W}_{NS}^{T}\boldsymbol{M}^{-1}(\boldsymbol{u}-\boldsymbol{h})+\dot{\boldsymbol{W}}_{NS}^{T}\dot{\boldsymbol{q}}. \quad (19)$$

The LCP has a unique solution for all vectors $\boldsymbol{b}$ if and only if the matrix $\boldsymbol{A}$ is a P-matrix [5]. However, even if $\boldsymbol{A}$ is not a P-matrix, the LCP may have unique solution for special choices of $\boldsymbol{b}$. For other choices of $\boldsymbol{b}$, Equation (18) may have no solution or multiple solutions.

Compliant contact models A general viscoelastic model for contact forces at the ith contact is given by

$$\lambda_{N,i}=f_{N,i}(\delta_{N,i})+g_{N,i}(\delta_{N,i},\dot{\delta}_{N,i}),\ i=1,\ldots,n_C, \quad (20)$$
$$\lambda_{T,i}=f_{T,i}(\delta_{T,i})+g_{T,i}(\delta_{T,i},\dot{\delta}_{T,i}),\quad i=1,\ldots,n_C, \quad (21)$$

where $f_{N,i}$ and $f_{T,i}$ are the elastic stiffness terms and $g_{N,i}$ and $g_{T,i}$ are the damping terms in the normal and tangential directions respectively. These functions depend on the geometry and material properties of the two bodies in contact and may be nonlinear. $\delta_{N,i}$ and $\delta_{T,i}$ are the local normal and tangential deformations. It is also necessary to model the frictional behavior of the contact. The details and variations on the compliant contact model and a range of frictional laws are discussed in [13].

The main advantages of the compliant contact model are that the inconsistencies with uniqueness and existence no longer arise and the contact forces are now uniquely determined even for the static indeterminate configurations. The disadvantage is that there is a need to extend the dimension of the state space from $2n-2(n_C+n_R)$ to $2n+n_C$.

4.2 Simulation approach

We adopt the integrated simulation framework proposed in [14] to combine the strengths of both the rigid body LCP model and the compliant contact model. This framework allows for on-line diagnostics that enable the automatic switching between models to maximize efficiency while avoiding ambiguous situations. The key step in this approach is to build the compliant contact state from the rigid body state variables when rigid body dynamics does not have a unique and stable solution for the contact forces. However, during the switch from the LCP formulation to the compliant contact model, it is necessary to ensure that the state of the system and the dynamic model are continuous [14].

5 Examples and results

5.1 A typical example

Consider the planar whole arm manipulation system shown in Figure 2. We assume that each arm (effector) of the manipulator has one contact point with the object. Σ_B is the base frame and Σ_i is the coordinate frame attached to the ith contact point. The following constraints on contact states are implied:

$$\begin{aligned} &n_R+n_S=4\\ &2n_R+n_S<7\\ &\text{rank}(\boldsymbol{W})=2n_R+n_S \end{aligned} \quad (22)$$

The first constraint says that the total number of contacts is four. The next two constraints essentially make the problem determinate. Clearly, these conditions are satisfied for the following three cases: (a) $n_R=2$, $n_S=2$; (b) $n_R=1$, $n_S=3$; and(c)$n_R=0$, $n_S=4$.

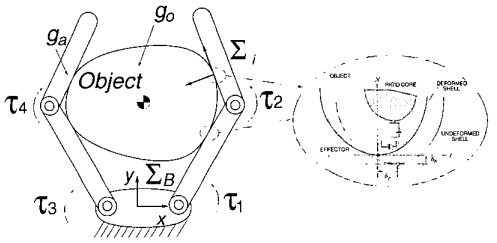

Figure 2: A planar whole arm grasp.

There are three different scenarios for this example. In the first scenario, Eq.(22) is satisfied and matrix $\boldsymbol{A}$ in Eq.(18) is a P-matrix. In this case the rigid body dynamic model is valid and solvable. In the second scenario, Eq.(22) is satisfied, but there are no guarantees on $\boldsymbol{A}$. In this scenario there is no unique solution for the contact forces and accelerations. This may happen for any of the three cases (a-c) above. Finally, in the third scenario, Eq.(22) is not satisfied. In this case, it is impossible to know what the contact forces are and therefore it is not possible to check for constraints on the contact forces. The $n_R=4$, $n_S=0$ case falls into this category. In the second and third scenarios, it is necessary to pursue a more complex model and as we argued before, the compliant contact model is the model of our choice for simulation.

5.2 Numerical results

In this subsection, we will use the scheme developed in Section 3 to control two frictional whole arm manipulation tasks with sliding constraints. In both tasks, the arms of a two 2-DOF manipulator is used to move an elliptical object in the horizontal plane with sliding contacts. The configuration of the system is depicted in Figure 2. This is the $n_S=4, n_R=0$ scenario discussed in the previous subsection. The Jacobian $\boldsymbol{J}$ of the manipulator is square for this scenario. The object used in the simulation has a major axis of 0.30m and its minor axis is 0.22m. The mass of the object is 1.69kg, and the moment of inertia about the center of mass is 1.46×10^{-2}kg·m^2. The fixed palm of the hand is 0.10m long. The length of each finger link is 0.20m. The mass of the finger link is 0.5kg with a centroidal moment of inertia of 1.67×10^{-3}kg·m^2.

The joints of the robot arm are driven by torque motors via the control law (11) designed to manipulate the object along a desired trajectory while maintaining the contacts. Although the grasp itself is statically indeterminate (four forces in the plane), because the torques are specified, the system is statically determinate. The rank of $\boldsymbol{W}_{\mu}\in\Re^{7\times4}$ remains four at all times. Since the system has three independent degrees of freedom, it is

easy to verify that the grasped object can be manipulated in three independent directions.

We first consider the situation when the rigid body model has a unique solution throughout the manipulation task. In the second example, we show the control results for the case when inconsistencies arise during the forward dynamics simulation. In both examples, the feedback gain matrices of the controller are chosen as the following to place all the poles of the error dynamics (14, 15) at -10:

$$K_p = 100 \cdot I_{3\times 3}, \quad K_v = 20 \cdot I_{3\times 3}, \quad K_\alpha = -10.$$

The force and position sensors are simulated with an $\pm 10\%$ additive random noise with uniform distribution. The compliant contact model used in both examples is Kelvin-Voigt model [13].

Example 1: LCP has a unique solution In the example, the manipulation task is to rotate the object from a 70 degree orientation to a 110 degree orientation in 1 second while keep its center of mass stationary. A fifth order polynomial is used to interpolate the desired orientation of the object. It can be shown that for this plan, if we choose $\mu = 0.1$ at all four contact points, the $\boldsymbol{A}$ matrix in the LCP formulation is always a P-matrix. The desired internal force magnitude is planned by solving the linear programming problem (17) with $\boldsymbol{\Lambda} = [0.5\ 0.5\ 0.5\ 0.5]^T$ which keeps the minimum normal contact forces at $0.5N$. The computed joint torque history based on (11) are shown in Figure 3(1).

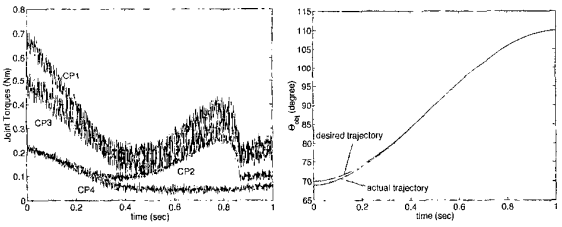

(a) Input joint torques (b) Object orientations

Figure 3: History of the input joint torques and the object orientations.

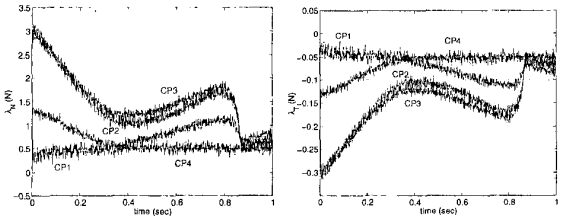

(a) Normal contact force. (b) Tangential contact force.

Figure 4: The contact force history (CP–Contact Point). The desired minimum normal contact force is 0.5N

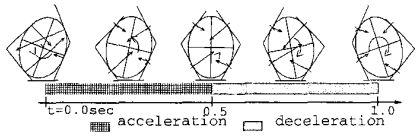

Figure 5: Snap shots of the system configuration.

The manipulation task can be simulated by either compliant model or the rigid body LCP model. The simulation results here are provided only for the rigid body LCP solution. Similar results are obtained by using the compliant contact model. The initial orientation is off by 1 degree. As seen from Figure 3(b), the control algorithm brings the object to the desired trajectory within 0.2sec., after which the actual and desired paths are virtually identical. Figure 5 shows the snap shots of the simulation results for system configurations. Figure 4 shows that the control algorithm stabilizes the minimum normal contact force around the desired value. Note that the contact force component that is at the threshold of 0.5N changes from contact point (CP) 1 to CP4 and then to CP2. This demonstrates the need for the planner (17). It is clearly not meaningful to simply design a controller that has $\lambda_{N,1}$ or $\lambda_{N,4}$ on its output variables.

Example 2: LCP does not always predict a unique solution In general, there is no guarantee that the LCP formulation has a unique solution for a frictional manipulation task. In such a case, it is impossible to use conventional simulation approach to validate the control algorithm. Consider the translation of the object from 0.12m to 0.15m in the vertical direction. If we set the coefficient of friction between the object and arm links 1 and 3 as $\mu_1 = 0.8$, and $\mu_2 = 0.6$ for links 2 and 4, the P-matrix condition is not always satisfied during the task. For example, at $t = 0.8$sec, the chosen coefficient of friction falls outside of the P-matrix region (Figure 7). The torque requirements for the four actuators are shown in Figure 6(a). Once again, as shown in Figures 6(b) and 8, the control algorithm converges both the force and motion trajectory to the desired paths in spite of the fact that the actual initial starting location is not on the desired trajectory.

The integrated approach is used to automatically switch the simulation flow between the rigid body LCP model and the CC (compliant contact) model.The dash lines in Figure 8 indicate such switching points between the models during the simulation. We can see that the integrated approach enables a continuous transition for the system dynamics when switching between models.

6 Concluding remarks

We have presented the control and dynamics of grasps using whole arm manipulation systems with rolling and sliding constraints. We developed a model based scheme that employs a minimal set of inputs to control the motion of the system while use the surplus inputs to regulate the internal forces and to maintain the contact interaction between the arms and the object. Since in general, the number of surplus inputs is less than the number of output force variables, we propose a controller that controls the critical contact force components. We address the use of contact models to achieve closed loop force control for systems with unilateral constraints. We

show that a simple compliant contact model, when used with the rigid body dynamic equations of motion, always yields a unique solution for the contact forces and is robust for the control purpose. While this model is superior to the traditional rigid body model in term of accuracy and consistency, it is also more complex and requires a larger number of parameters. To resolve this problem, we use a previously developed general simulation platform that integrates the compliant contact model and the rigid body LCP model to maximize computational efficiency without compromising accuracy. The complete methodology, from the control algorithm, the contact models, to the simulation framework is demonstrated on a planar whole arm manipulation system. Numerical results show the robustness of the control scheme as well as the integrated simulation platform.

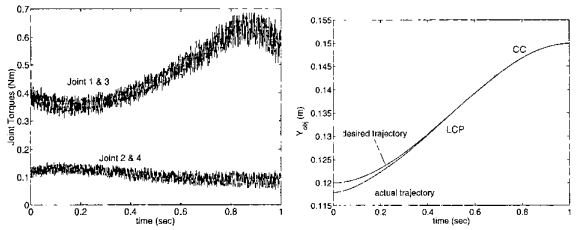

(a) Input joint torques (b) Object displacement

Figure 6: An elliptical object being translated in the positive y-direction with four sliding contacts.

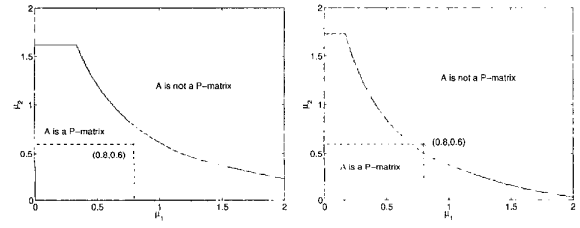

(a) t=0.4sec (b) t=0.8sec

Figure 7: μ-space plots at different times.

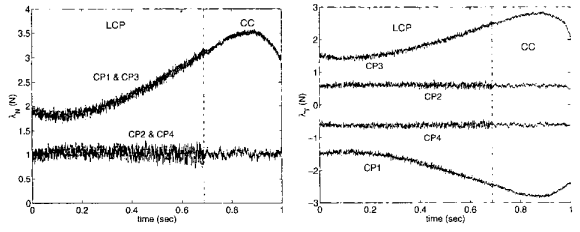

(a) Normal contact force. (b) Tangential contact force.

Figure 8: The contact force history. The desired minimum normal contact force is 1N.

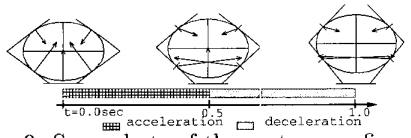

Figure 9: Snap shots of the system configuration.

Acknowledgments

We gratefully acknowledge the support of NSF grants CISE RI 9703220 and ARO grant MURI DAAH04-96-1-0007.

References

[1] A. Bicchi, C. Melchiorri, and D. Ablluchi. the mobility and manipulability of general multiple limb robots. *IEEE Trans. Rob. Automat.*, 11(2):215–228, 1995.

[2] L. Cai and A. A. Goldenberg. An approach to force and position control of robot manipulators. In *Proc. IEEE Int'l Conf. Robot. Automat.*, pp. 86–91, May 1990.

[3] A. Cole, J. Hauser, and S. Sastry. Kinematics and control of multifingered hands with rolling contact. *IEEE Trans. Automat. Contr.*, 34(4):398–404, Apr. 1989.

[4] A. Cole, P. Hsu, and S. Sastry. Dynamic control of sliding by robot hands for regrasping. *IEEE Trans. Rob. Automat.*, 8(1):42–52, Feb. 1992.

[5] R. W. Cottle, J. S. Pang, and R. E. Stone. *The Linear Complementarity Problem.* Academic Press, Inc., San Diego, CA, 1992.

[6] L. Han and J. C. Trinkle. The instantaneous kinematics of manipulation. In *Proc. IEEE Int'l Conf. Robot. Automat.*, pp. 1944–1949, 1998.

[7] P. Hsu. Coordinated control of multiple manipulator systems. *IEEE Trans. Rob. Automat.*, 9(4):400–410, Aug. 1993.

[8] O. Khatib. A unified approach for motion and force control of robot manipulator: The operational space formulation. *IEEE J. Rob. Automat.*, RA-3(1):43–53, Feb. 1987.

[9] V. Kumar and K. J. Waldron. Actively coordinated vehicle systems. *ASME J. Mech., Transm., and Automat.*, 111(2):223–231, June 1989.

[10] P. Lötstedt. Analysis of some difficulties encountered in the simulation of mechanical systems with constraints. Technical report, NADA - The Royal Institute of Technology, Stockholm, Sweden, 1979. TRITA-NA-7914.

[11] K. Mirza and D. E. Orin. General formulation for force distribution in power grasp. In *Proc. IEEE Int'l Conf. on Robotics and Automation*, pp. 880–887, 1994.

[12] E. Paljug, X. Yun, and V. Kumar. Control of rolling contacts in multi-arm manipulation. *IEEE Trans. Rob. Automat.*, 10(4):441–452, Aug. 1994.

[13] P. Song, P. Kraus, V. Kumar, and P. Dupont. Analysis of rigid body dynamic models for simulation of systems with frictional contacts. *ASME J. Appl. Mech.*, 2000. To appear.

[14] P. Song, M. Yashima, and V. Kumar. Dynamic simulation for grasping and whole arm manipulation. In *Proc. IEEE Int'l Conf. Robot. Automat.*, pp. 1082–1087, Apr. 2000.

[15] J. Trinkle, J.-S. Pang, S. Sudarsky, and G. Lo. On dynamic multi-rigid-body contact problems with coulomb friction. *Zeitschrift fr Angewandte Mathematik und Mechanik*, 77(4):267–280, Apr. 1997.

[16] Y.-T. Wang and V. Kumar. Simulation of mechanical systems with unilateral constraints. *ASME J. Mech. Design*, 116(2):571–580, June 1994.

[17] T. Yoshikawa. Control algorithm for grasping and manipulation by multifingered robot hands using virtual truss model representation of internal force. In *Proc. IEEE Int'l Conf. Robot. Automat.*, 2000.

[18] X. Yun and V. Kumar. An approach to simultaneous control of trajectory and interaction forces in dual arm configurations. *IEEE Trans. Robot. Automat.*, 7(5):618–625, 1991.